LRP 429/91 May 1991

IDEAL TOROIDAL STABILITY β-LIMITS AND SHAPING EFFECTS FOR RESERVED FIELD PINCH CONFIGURATION

R. Paccagnella, A. Bondeson, H. Lütjens

Ideal toroidal stability β limits and shaping effects for Reversed Field Pinch Configurations

R. Paccagnella

Istituto Gas Ionizzati
Consiglio Nazionale delle Ricerche
Associazione EURATOM-CNR-ENEA
Corso Stati Uniti, 4
I-35020 PADOVA
Italy

A. Bondeson, H. Lütjens

Centre de Recherches en Physique des Plasmas,
Association Euratom-Confédération Suisse,
Ecole Polytechnique Fédérale de Lausanne,
21 Avenue des Bains,
CH-1007 LAUSANNE
Switzerland

Abstract: The influence of shaping and toroidicity on the ideal MHD stability of the Reversed Field Pinch (RFP) is investigated both with respect to current and pressure driven modes. It is found that triangularity and x-point shaping does not significantly modify the operational limits of RFP, while ellipticity and D-shaping is destabilizing. A simple relation for the stability of current driven modes is also given.

submitted to Nuclear Fusion

1. Introduction

The ideal MHD stability of the Reversed Field Pinch (RFP) is rather well understood in the cylindrical approximation [1,2]. However, the importance of toroidal effects has not been given much attention theoretically and even less is known about the effect of shaping on RFP performance. The purpose of the present investigation is to study these issues by means of numerical computation using two dimensional toroidal equilibrium and stability codes. The parametrization of the equilibrium has been chosen so as to make possible a meaningful comparison with previous stability analyses [3,4] of the RFP in cylindrical geometry. The aspect ratio has generally been chosen R/a=4 motivated by the design of the RFX experiment in Padova.

In the first part of the work the effect of toroidicity on current and pressure driven modes for a circular RFP has been considered. For the circular RFP at zero β, we recover the cylindrical limits; these modes are not much affected by toroidal effects.

Moreover enhancing the β, for current driven stable configurations, has the effect to destabilize pressure driven localized interchange modes of the Mercier type [5]. They seem also, as expected for circular plasma section [6], not much affected by toroidal effects. It is interesting to note that for realistic RFP configurations the ideal β limits set by these Mercier modes are in the range $10 \div 15$ %, which is in the same range as the β values observed in experiments [7]. The limiting role played by the Mercier modes differs from the condition in tokamaks, where the β limit is due to ballooning instabilities [8], or "ballooning-like" low n modes [13].

Here, we have considered the circular RFP as a reference case, actually the most important part of the work has dealt with the effect of shaping on stability. We have considered four different plasma shapes: elliptic, triangular, D-shaped and also " x-point" like sections.

A first result of the computations is that the plasma shaping has little effect on current driven modes, although ellipticity is slightly destabilizing. A very simple criterion for the stability of m=1 current driven modes in terms of macroscopic quantities has been also found. Moreover it seems not to be possible to enhance the β limits using ellipticity, triangularity or D shapes, probably due to the average

bad curvature of the RFP [9]. Although this rather pessimistic result is not completely unexpected, our study shows an important difference between RFP and tokamak. It appears that in an RFP, shaping does not give access to more favorable regions of operating space (such as the increased current capability of the tokamak) where the β limit could be increased.
Concerning the "x-point" like configurations, we find that they do not affect appreciably the current driven stability boundaries and also the ideal β limits obtained for the circular cross section, at least if the "x-point" is positioned inside the torus. This result can be considered interesting for future RFPs with divertors. Obviously a question which has been not addressed by the present computations, is the effect of an x-point on the destruction of magnetic surfaces and on the related stochastic transport. This represents an important topic to be clarified.
The paper content is organized as follows: section 2 deals with the equilibrium parametrization, section 3 with the stability for the circular case, and finally section 4 presents the results of shaped plasma cross sections.

2. Equilibrium parametrization

In this study we have used the equilibrium code CHEASE [10] for solution of the Grad-Shafranov equation and the toroidal stability code MARS [11].
The Grad-Shafranov equation allows the specification of two profiles. We have chosen to specify p and $T=RB_\phi$ as function of poloidal flux Ψ.
In order to facilitate the comparison with previous results [3,4], the following parametrization has been chosen for the T profile:

$$T = T(o) - R_o \int \mu \, ds \qquad (2.1\ a)$$

with

$$\mu = \mu\,(o) \cdot (\,1 - s^{\alpha}) \qquad (2.1\ b)$$

where $s=1-\Psi/\Psi_{min}$ is the radial coordinate with s=0 on the magnetic axis, s=1 on the plasma-vacuum boundary and R_o is the radius of the plasma magnetic axis.
In the cylindrical limit this parametrization gives:

$$B_\phi(\Psi) = \frac{T}{R_0} = B_\phi(o) + \mu(o)\left(-s + \frac{s^{\alpha+1}}{\alpha+1}\right) \qquad (2.2)$$

and

$$q(o) = -\frac{2\Psi_{min}}{R_0 B_\phi(o)} \frac{1}{\mu(o)}$$

Note that the value of q(o) can be known only a posteriori, after the Grad-Shafranov equation has been solved and Ψ_{min} , $B_\phi(o)$ are determined. In the cylindrical case [3], $\mu(o)\, a = 2\,\Theta_o$ (a being the plasma minor radius), was directly connected with q(o):

$$q(o) = \frac{2}{R\,\mu(o)} = \frac{a}{R\Theta_0} \qquad (2.3)$$

Actually (2.3) can be taken as a definition of Θ_o. In this way the results presented here can be compared with the previous, for example in terms of stability plots in the α–Θ_o plane.
Obviously the parametrization (2.1) for μ resembles the cylindrical case although with some differences. In fact, while previously μ was a function of minor radius r [3], now it is a function of Ψ. In the next section we shall see that this produces only a small effect on the equilibria. More importantly, with finite pressure our choice of μ (2.1b) connects the poloidal current to the poloidal field, while in the definition used in [3,4] μ is related to the field aligned current $\mu = \mathbf{J}\cdot\mathbf{B}/B^2$.
Another point which can be useful to remark is that setting in (2.2) $B_\phi(1)=0$ the following relation is obtained:

$$\mu(o) = B_\phi(o)\left(1 + \frac{1}{\alpha}\right)$$

This equation represents the marginal curve at which the magnetic field is zero at the wall. For values of $\mu(o)$ above this curve the reversal point is inside the wall, on the opposite case the toroidal field is not reversed.
It is also necessary to specify a function for the pressure, $p(\Psi)$. The pressure profile has been chosen as follows:

$$p = c\,(1-4\,s^3+3\,s^4) \qquad (2.4)$$

This gives p=0 on the boundary and p' = dp/dΨ vanishes linearly on the boundary and quadratically on the magnetic axis. This choice corresponds to a quite broad pressure profile, as is optimal for the Mercier criterion which becomes rather restrictive in the central region.

2.2 F and Θ for RFPs with arbitrary shape

In describing RFPs configurations, two important parameters are:

$$F = \frac{B_\phi^w}{\langle B_\phi \rangle} \qquad \Theta = \frac{B_p^w}{\langle B_\phi \rangle} \qquad (2.5)$$

where $B_\phi{}^w$ and $B_p{}^w$ are the toroidal and poloidal magnetic fields at the plasma wall.
For an RFP configuration with an arbitrary shape the previous expressions have been generalized and the the following definitions have been taken:

$$B_{\phi,p}^w = \frac{\int_{\delta\Omega} B_{\phi,p}\, dl}{\int_{\delta\Omega} dl}$$

$$\langle B_\phi \rangle = \frac{\int_\Omega B_\phi\, ds}{\int_\Omega ds}$$

where $\delta\Omega$ is the plasma boundary and Ω the plasma domain.

3. Stability for the circular RFP

In order to show more quantitatively the differences between the toroidal parametrization (2.1) and the cylindrical case [3], we plot in Fig.1 the toroidal equilibria as points (triangles) in the cylindrical F-Θ diagram. The toroidal profiles are computed for an aspect ratio R/a = 4. The F-Θ curves are practically indistinguishable for Θ and F in the experimentally interesting domain, while the toroidal curves depart from the cylindrical ones at high values of Θ.
The following stability calculation assume a free-boundary plasma surrounded by a vacuum region of 10% of the minor radius.

3.1 Force-free stability analysis

The stability diagram in Θ_o - α plane obtained in the cylindrical limit [3] is shown in Fig.2.
Firstly, we have checked that the stability boundaries on the bottom, due to external (m=1) modes, and on the right, due to internal (m=1) modes, are not modified by toroidal effects. Here the words: "external" and "internal" refer to whether the resonance surface of the mode is outside or inside the field reversal [3]. Note that this is somewhat different from the standard distinction, since these expressions are usually used to identify modes which remain unstable (internal) or are stabilized (external) in the case of fixed boundary. In the present free-boundary calculation we use the terminology internal and external in the sense of ref. [3]. We remark however that both tyes of modes (internal and external resonant) are influenced by both wall boundary conditions and wall position, although the internal resonant modes seem somewhat less sensitive [12].
In Fig.3a,b the growth rates (normalized to the Alfvén time) vs. α and vs. Θ_o for internal and external modes respectively, are shown. The marginal point corresponds almost exactly for both cases with the stability boundary of Fig.2, as can be easily checked.
In the same figure it is also shown that the growth rates are independent of the aspect ratio, in fact the circles refer to R/a=4 and the crosses to R/a=10.
In Fig.4 the particular structure of the internal m=1 current driven modes is shown. The displacement is peaked near the resonance

surface, wheres the radial component of the magnetic field takes its maximum near the wall, outside the resonance.
Moreover there is almost no toroidal coupling between different poloidal harmonics, in fact the contributions to the eigenfunctions for $m \neq 1$ are very small. We therefore conclude that current driven modes are almost unaffected by toroidal effects (as is, at least approximately, true also for tokamaks).

3.2 Pressure driven modes

As a first general observation concerning pressure driven modes we remark that the marginal stability is set by interchange modes of the Mercier type. In Fig.5 the marginal average β for stability is plotted vs. Θ_0 for a fixed α. The curve corresponds just to the stabilization of ideal interchange modes.
The stability is only slightly affected by toroidicity. This is as expected: for example, the Yurchencko-Shafranov analysis [6], for a circular low β tokamak shows only a slight alteration of the Suydam criterion (represented by the $(1-q^2)$ factor in (3.1)):

$$\frac{1}{4}\left(\frac{q'}{q}\right)^2 + \frac{2\mu_0 p'}{r B_\phi^2}\,(1 - q^2) \geq 0 \qquad (3.1)$$

This can be also seen in Fig.5, in which the same boundary for stability has been found for two aspect ratios: R/a=4,10.
Moreover from Fig.5 it is possible to see that for typical RFP configurations ($1.5 \leq \Theta_0 \leq 1.7$) the average β limit is in the range 10 ÷ 15 %, and therefore comparable with the experimental values [7].
The sharp stability boundary in Fig.5 at $\Theta_0 = 1.9$, is set by the external current driven modes. However this boundary corresponds to very unlikely configurations in terms of F and Θ (F<-2, Θ>3). The behavior of the growth rates vs. β (above the Mercier's stability limit) is represented in Fig.6 for two values of α. The growth rates are much lower than those corresponding to current driven modes, but still appreciable; they increase with β and are little affected by the current profile. Moreover in Fig.7 the radial component of velocity eigenfunction (a) and magnetic field (b) for a case with $<\beta>=30\%$ are shown. A toroidal coupling between different harmonics is present. The eigenfunctions are normalized to the maximum of

m=1 mode, so that it is clear from the figure that m=0,1 are the predominant modes.
When the β limit due to interchange modes is violated the unstable spectrum extends to high n values and localized modes are destabilized with relatively high (of the order of 10^{-1}) growth rates. The limiting role of the interchange modes is different from the tokamak case, where the ballooning modes are normally destabilized below the Mercier limit, at least in the high-shear region with q well above unity.

4. Shaping of plasma cross section

In an attempt to improve the current driven and β limits due to ideal modes, we have considered shaping of the plasma cross section.
It is well known for the tokamak that producing an elliptic plasma has the effect to enhance the current limit imposed by the $q_s > 2$ limit and also that plasma shaping produces a beneficial effect on β limits [13] when the shape is such that the field lines spend most of the time in the good curvature region.
The stabilizing effect of shaping for RFP, at least on pressure driven modes, could a priori be expected to be not so strong as in tokamak, due to the fact that the toroidal favorable curvature in the pinch is much smaller than in tokamak like configurations. Nevertheless, as a systematic study of the effect of shaping on both current driven and pressure driven modes has been never done for RFP like configurations, many questions concerning the effects of shaping on the operational limits are open.
We have considered four types of plasma shapes:

(a) triangular cross-section;

(b) elliptic cross sections;

(c) D shaped cross sections;

(d) "x-point" like configurations;

In the following sections the results in terms of stability boundaries for current driven modes and β limits for stability are presented for these different equilibria.

4.1 Elliptic, triangular and D shaped RFP plasmas

The shape of the boundary is described by the following equations:

$$r = R_0 + R_0 \varepsilon \cos(\theta + \delta \sin(\theta))$$
$$z = R_0 \varepsilon E \sin(\theta)$$

where r and z are the cartesian coordinates with the origin at the center of the torus, R_0 is the major radius, ε is the inverse of the aspect ratio, E and δ are the ellipticity and triangularity, respectively. First, we have examined the current driven stability limits at zero β. The results for triangular, elliptic, D shaped and the reference circular case are plotted in Fig.8 in the F-α plane. The aspect ratio is fixed at R/a=4. The stability region for internal current driven modes extends on the right of the curves plotted in Fig.8. The curve marked with triangles corresponds to the boundary for circular and triangular (δ = 0.4) cross sections. The curve marked with white circles corresponds to the elliptic deformed plasma shape (E = 1.6) , and that marked with black circles to the D shaped cross section (E=1.6, δ =0.4). Note that in Fig.8 we have chosen to represent the stability boundaries in the F-α plane rather than in the Θ_0- α plane. This choice is motivated by the following two points. First, in the toroidal computations Θ_0 is not an input parameter, as it was in the cylindrical case. The second consideration is connected to the fact that for different plasma shapes, the same values of F and Θ correspond to different values of Θ_0 . So in order to compare similar configurations in terms of the "physical" parameters F and Θ it is necessary to represent the stability boundaries in a different way with respect to the cylindrical case. Moreover this has the advantage to limit the analysis to a "reasonable" region of the parameter space.
Fig.8 shows that triangularity does not affect the circular stability boundary: it is neither stabilizing nor destabilizing. This is not the case for elliptic sections. In fact, for elliptically deformed cross sections, the stability boundary is shifted at higher α's (for a fixed F value), i.e. the effect is destabilizing. The same is true for D shaped cross sections.
Fig.9 shows the F-Θ curves computed at α values corresponding to marginal stability for the different shapes. The effect of shaping on the F-Θ curves is very small. Moreover we note that the stability boundaries are determined (as in the circular case) by internal resonant m=1 modes (although now some toroidal coupling with m=0

modes is also present). The resonance surface for these modes is near the magnetic axis and for the aspect ratio (4) considered here they have toroidal periodicities in the range $6 \leq n \leq 8$.
Our main conclusion is that shaping has a small influence on stability of internal current driven modes, although some destabilization is observed for elliptic plasma section. In Fig.9 the straight line shows the effect of pressure (for $<\beta> = 10\%$) on the stability boundary for a circular cross-section. As can be seen the change in the current profile due to pressure is more affecting the stability than shaping does.
The stability boundary due to "external" current driven modes (Fig.2) has been also checked to be unaffected by shaping, but it must be noted that this boundary corresponds to quite unrealistic values of F (≤ -2) and Θ (≥ 3).
In examining the effect of shaping on pressure driven modes, we have considered triangular cross section.
Similar to the case for the current driven modes we find that triangularity does not destabilize the pressure driven modes.
A plot of γ vs. $< \beta >$ for two configurations with different but rather small α values (near the marginal point for $\beta = 0$ stability) is shown in Fig.10. Three different observations can be made: first the shaping has no effect, in fact the curves for the circular and the triangular case overlap completely; second the stability β limit is due to localized interchange Mercier's modes (the arrow in the figure) and it is also independent of shaping; third the $<\beta>$ threshold for the destabilization of low n "current driven " like modes increases with α, but again it is unaffected by shaping.
Fig.9. shows that the stability limit for internal m=1 modes is represented quite well by the following relation:

$$\Theta \leq -F + \Theta_{rev}$$

where $\Theta_{rev} \approx 1.5$ corresponds to the value of Θ at which F=0.
This expression can be easily transformed into:

$$\mu_o I \leq 2\pi a \left[-B_\phi(a) + \Theta_{rev} \langle B_\phi \rangle\right]$$

where I is the total toroidal current, a is the plasma minor radius and $< B_\phi >$ is the average toroidal flux.
In other terms the internal m=1 ideal modes are setting a limit for the current which can be expressed in a simple way as a function of externally controlable parameters. We point out that the

experimental points, for example for η-β II, lie approximately in the region between the zero β curve and the stability boundary obtained with 10% β represented also in Fig.9.

4.2 "X-point" like configurations

This kind of configuration is interesting in the perspective to build an RFP with a divertor.
The following parametrization describe the "x-point" like boundary:

$$r = R_b + R_b \varepsilon f(\theta) \cos(\theta)$$

$$z = R_b \varepsilon f(\theta) \sin(\theta)$$

with $f(\theta)$ given by:

$$f(\theta) = 1 + \frac{\sigma}{1 + \frac{\left[\sin^2\left(\frac{\alpha-\alpha_0}{2}\right) + \zeta\right]^{\nu}}{\Delta}}$$

Note that the x-point has been approximated numerically by a rounded of corner (see Fig.11) due to numerical difficulties in dealing with a real hyperbolic point, where the flux coordinate system becomes singular.
First the current driven modes stability has been tested. The "x-point" was positioned at $\theta = 3/4\ \pi$, but we find that the current driven stability boundary was unaffected by the position of the x point. The stability region with respect to the circular case is not affected and is again represented in the F-α plane by the curve marked with triangles of Fig.8. This result has been obtained with the following choice for the parameters determining the sharpness of the "x-point": $\sigma = 1.2$, $\nu = 0.45$, $\Delta = 0.6$, $\zeta = 3\ 10^{-3}$. This corresponds to a rather rounded corner.
Concerning the β limits for stability it is well known for the tokamak [14] that the position of the x-point affects the β limits and that the best results are obtained when the x-point is inside the torus, in the region of good curvature. Therefore in Fig.12 the β limits for the stability of Mercier modes, are plotted against the position of the "x-

point". Although the effect is not extremely strong, there is a clear indication that when the "x-point" is inside the torus, the β limits are higher, in complete analogy with tokamaks. Note also that in the range $3/4\ \pi \leq \theta \leq 5/4\ \pi$, the limits are the same as the circular case represented by the arrow in the figure.

Conclusions and discussion

In this work we have studied the stability of RFPs against ideal current and pressure driven modes for axisymmetric configurations with shaped cross sections.
Our main conclusions is that both toroidicity and shaping have small influence on ideal current driven modes boundaries and β limits for stability. Cross-sections with triangular deformation and also "x-point" like configurations, neither improve nor deteriorate the stability, while ellipticity is destabilizing. Thus, our results concerning x-point show that from the ideal MHD point of view RFPs with divertors should work. However some important topics as the effect of shaping on magnetic braiding cannot be addressed by the simple model of linear ideal MHD.
The ideal β limits obtained for realistic configurations (F and Θ in the experimental domain) are of the order of 10 ÷ 15 %, which is in the same range as experimental results. The theoretical β limits are not influenced by shaping. However in the case of "x-point" like configurations, it is necessary to locate the "x-point" inside the torus to recover the circular β limits .
The result that shaping has no influence on stability of current driven modes and ideal β limits has been obtained for a given class of equilibria. However it is clear that if shaping would either modify the class of achievable equilibrium states or would shift the operation points in the F-Θ plane, both current driven and β limits would probably change. Thus the question of the usefulness of shaping for RFP like plasma confinement can be conclusively answered only by performing real experiments! Some already existing experimental results [15,16] are not contradictory with the conclusions of the present theoretical investigation, in fact these shaped RFP plasmas show similar performances as circular RFPs.
Another interesting result of this paper is that the stability of internal m=1 ideal modes set a very simple constraint on the current. This limit can be expressed in terms of externally tunable parameters. Moreover from a comparison with experimental data, we have found that RFPs seem to operate near this limit.

A question which has been not addressed in the present work is the problem of stability in presence of finite plasma resistivity. On the basis of cylindrical computations it is known that the operational limits set by the current driven modes are slightly affected by resistivity when the wall position is just on the plasma surface [3], but that it has a strong destabilizing effect when the wall is moved away from the plasma [2,12]. Therefore it could be important to investigate the effect of resistivity on current driven modes in presence of toroidicity and/or shaping for a free-boundary plasma model. We leave this subject for future studies.
Instead as concerns the pressure driven modes there is a basic difficulty in defining β limits in presence of resistivity, in fact when $q<1$, resistive interchange modes are unstable even at very low pressure. On the other hand these modes are so localized, especially at high plasma conductivity, that they are probably affecting the β only in an indirect way through complicate transport mechanisms. Therefore the analysis has been restricted to ideal modes, which are generally agreed to play a fundamental role in setting the β limits also for tokamaks [17].

Acknowledgements:

One of the authors (R.P) thanks Euratom authorities for providing mobility funds to support this study and CRPP, where this work was carried out, for offering kindly hospitality.

References

[1] ROBINSON D.C., Plasma Phys. **13** (1971) 439.
[2] ROBINSON D.C., Nucl. Fusion **18** (1978) 939.
[3] ANTONI V., MERLIN D., ORTOLANI S., PACCAGNELLA R., Nucl. Fusion **26** (1986) 1711.
[4] MERLIN D., ORTOLANI S., PACCAGNELLA R., SCAPIN M., Nucl. Fusion **29** (1989) 1153.
[5] MERCIER C., Nucl. Fusion **1** (1960) 47.
[6] SHAFRANOV V.D., YURCHENKO E.I., Soviet Phys. JETP **26** (1968) 682.
[7] ANTONI V., BUFFA A., CARRARO L., et. al., in Controlled Fusion and Plasma Physics (Proc. 14th Eur. Conf. Madrid, 1987), Vol.11D, Part II, European Physical Society (1987) 532.
[8] WESSON J.A., SYKES A., Nucl. Fusion **25** (1985) 85.
[9] FREIDBERG J. P., "Ideal Magnetohydrodinamics", ed. Plenum Press

(1987).
[10] LüTJENS H., BONDESON A., ROY A., CRPP Internal Report LRP 405/90, submitted to Comp. Physics Communication.
[11] BONDESON A., VLAD G., LüTJENS H., in Controlled Fusion and Plasma Physics (Proc. 17th Eur. Conf. Amsterdam, 1990), Vol. II, p.906.
[12] MERLIN D., ORTOLANI S., PACCAGNELLA R.,in Controlled Fusion and Plasma Physics (Proc. 14th Eur. Conf. Madrid, 1987), Vol.11D, Part II, European Physical Society (1987) 442.
[13] TROYON F., GRUBER R., SAURENMANN H., SEMENZATO S., SUCCI S., Plasma Phys. **26** (1984) 209.
[14] BISHOP C.M., Nucl. Fusion **26** (1986)1063.
[15] OOMENS A.A.M., LASSING H.S., VAN DER MEER A.F.G., "Reversed Field Pinch discharges with elongated minor cross-section", Rijnhuizen Internal Report 90-197 (1990).
[16] ALMAGRI A., et al., Nucl. Fusion **27** (1987) 1795.
[17] TROYON F., GRüBER R., Phys. Lett. A, **110** (1985) 29.

Figure Captions

Fig.1 F vs. Θ curves at different α's. Lines correspond to cylindrical states and triangles show the toroidal states with R/a=4.

Fig.2 Θ_o vs. α diagram showing the stability boundaries.

Fig.3a γ vs. α plot for n=8 internal mode. Circles refer to R/a=4 and crosses to R/a=10. (Θ_o is fixed to 2).

Fig.3b γ vs. Θ_o plot for an n=4 external mode. Circles correspond to R/a=4 and crosses to R/a=10 (α is fixed to 4).

Fig.4 Radial component of velocity (circles) and magnetic field (crosses) eigenfunctions for an m=1, n=8 internal mode (Θ_o=2, α=2.1). The functions are normalized to their own maximum value. The arrow indicates the resonance radius.

Fig.5 $<\beta>$ limit for stability of Mercier's modes at different Θ_o for α=4. Circles refer to R/a=4 and crosses to R/a=10.

Fig.6 γ vs. $<\beta>$ for two different values of α (R/a=4).

Fig.7 Radial component of velocity (a) and magnetic field (b) eigenfunctions. The equilibrium corresponds to α=6, Θ_o= 1.45 and $<\beta>$=30%. The mode has n=15. The different harmonics are normalized to the maximum of the m=1 mode.

Fig.8 F vs. α stability boundaries. The stable region is on the right of the different curves. Triangles refer to circular and triangular shaped cross sections (δ =0.4), full circles to D shaped sections (δ =0.4, E=1.6) and open circles to elliptic plasma shape (E=1.6). R/a is fixed to 4.

Fig.9 F vs. Θ states corresponding to the marginal stability curves of Fig.8. Continous line represents the boundary for initial equilibria with $<\beta>$ = 10%.

Fig.10 γ vs. $<\beta>$ for two different values of α near the stability boundary for circular (circles) and triangular (crosses) sections. The mode is the internal n=7. The arrow indicates the Mercier limit.

Fig.11 "x-point" like cross section.

Fig.12 $<\beta>$ limit due to interchange modes vs. the poloidal angle θ. The arrow indicates the circular limit. (α is fixed to 4).

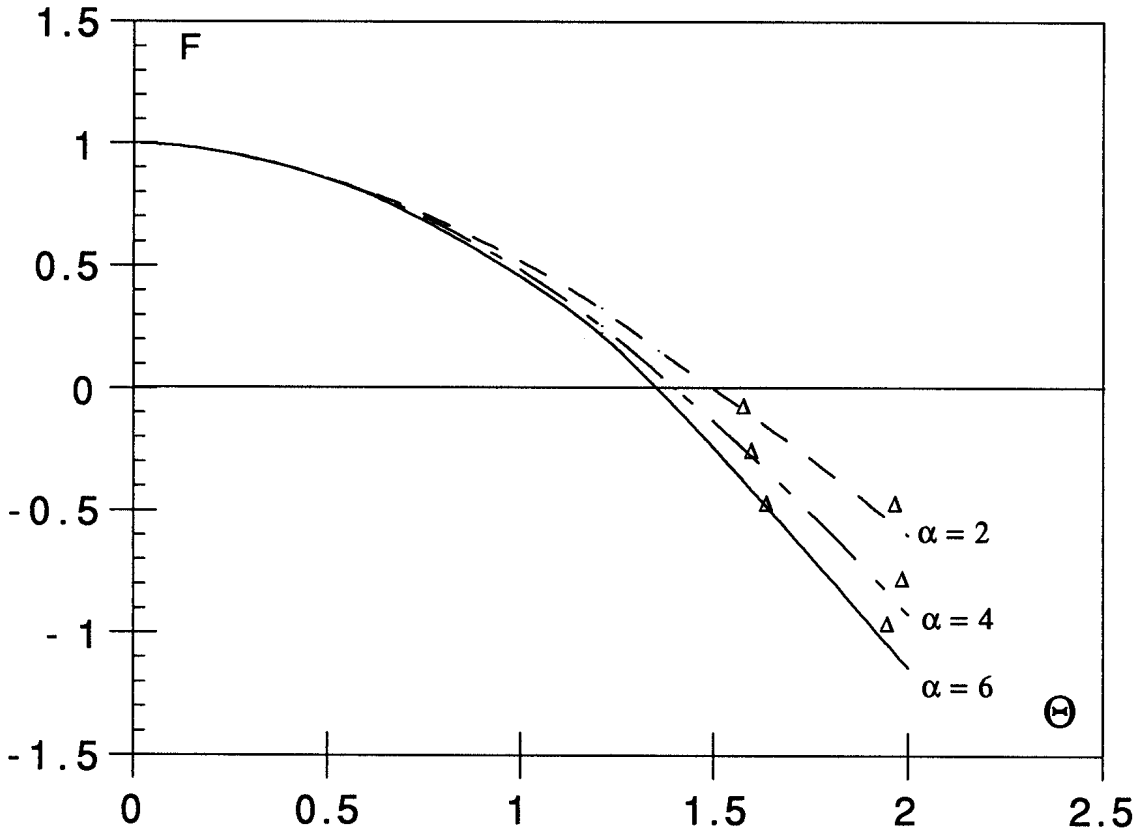

Fig.1

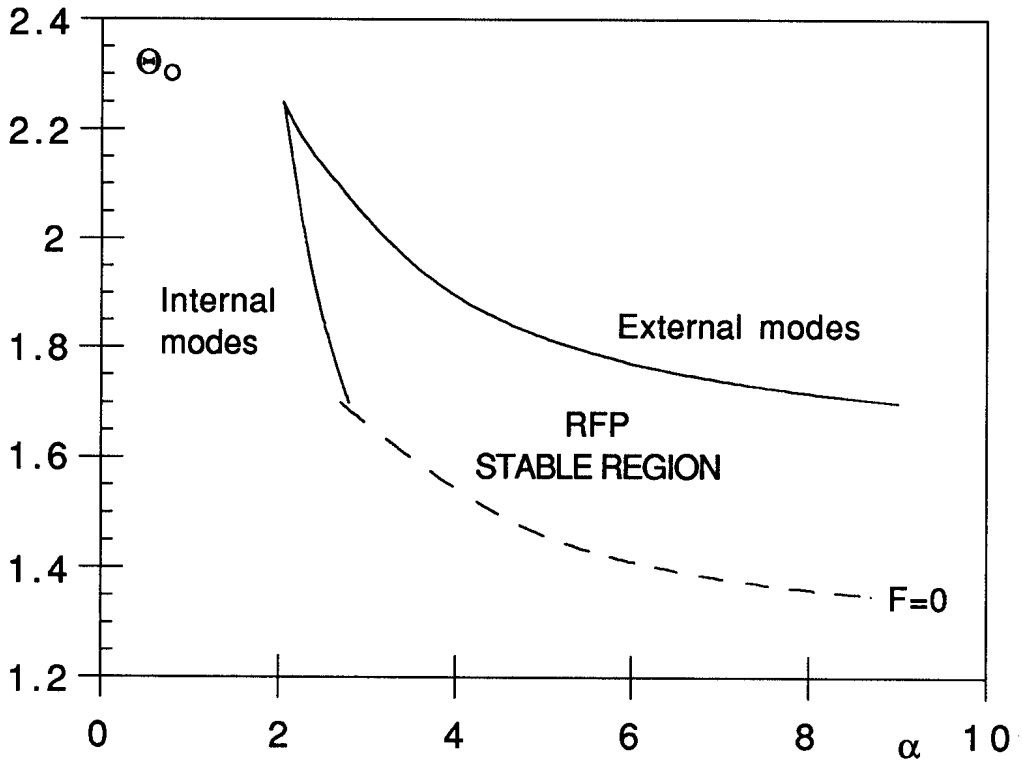
2.4
2.2
2
1.8
1.6
1.4
1.2
Θ_o
Internal
modes
External modes
RFP
STABLE REGION
F=0
0
2
4
6
8
α
10

Fig.2

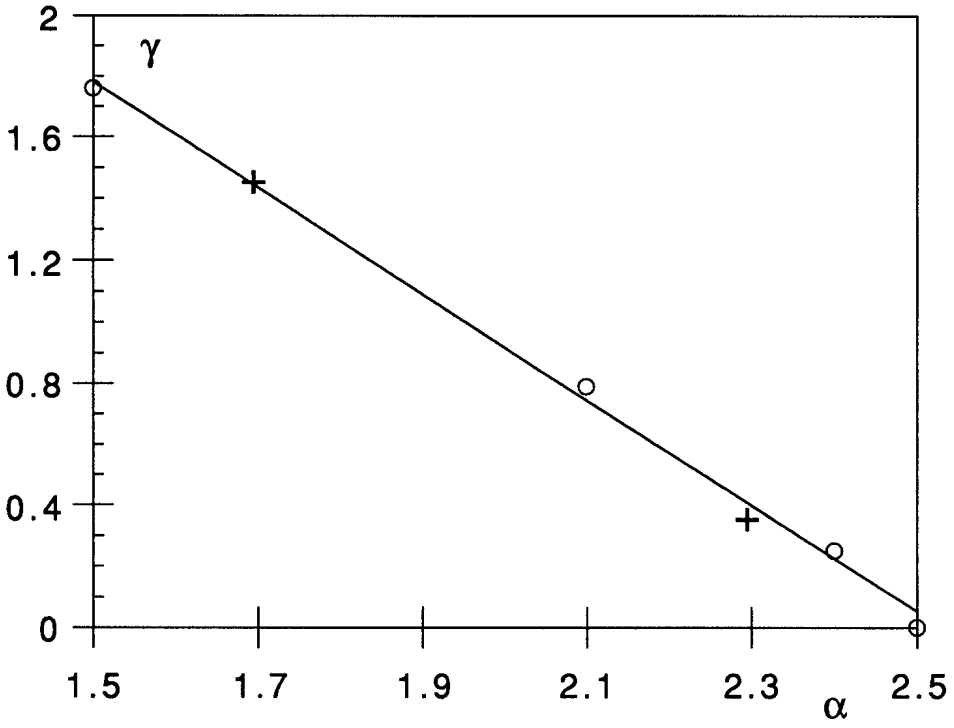
2
γ
1.6
1.2
0.8
0.4
0
1.5
1.7
1.9
2.1
2.3
2.5
α

Fig.3a

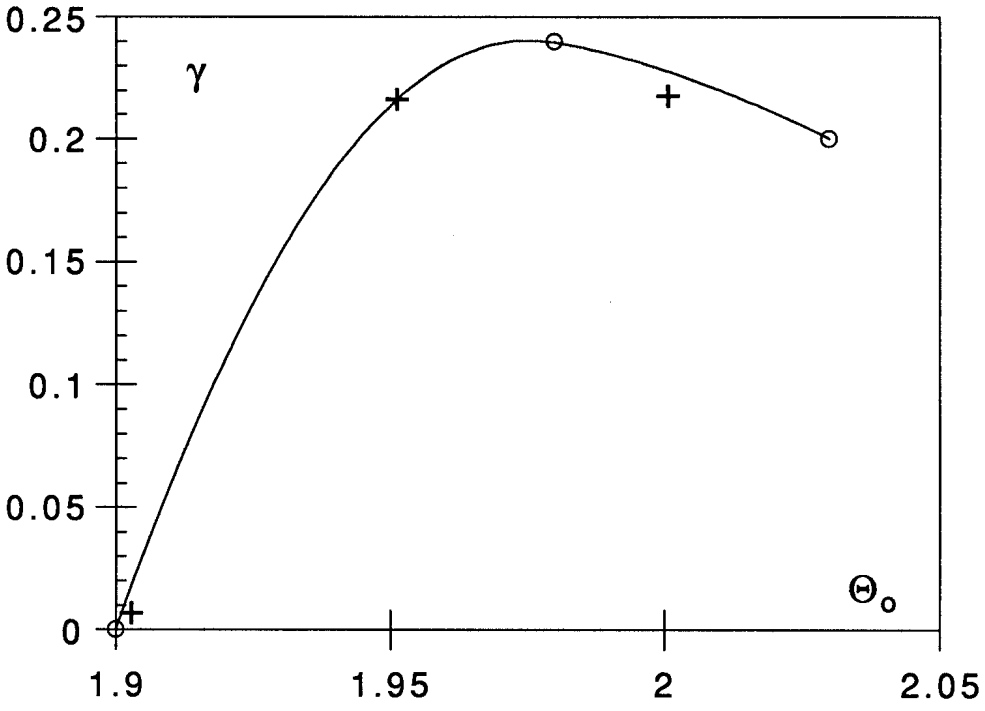
0.25
γ
0.2
0.15
0.1
0.05
0
1.9
1.95
2
2.05
Θo

Fig.3b

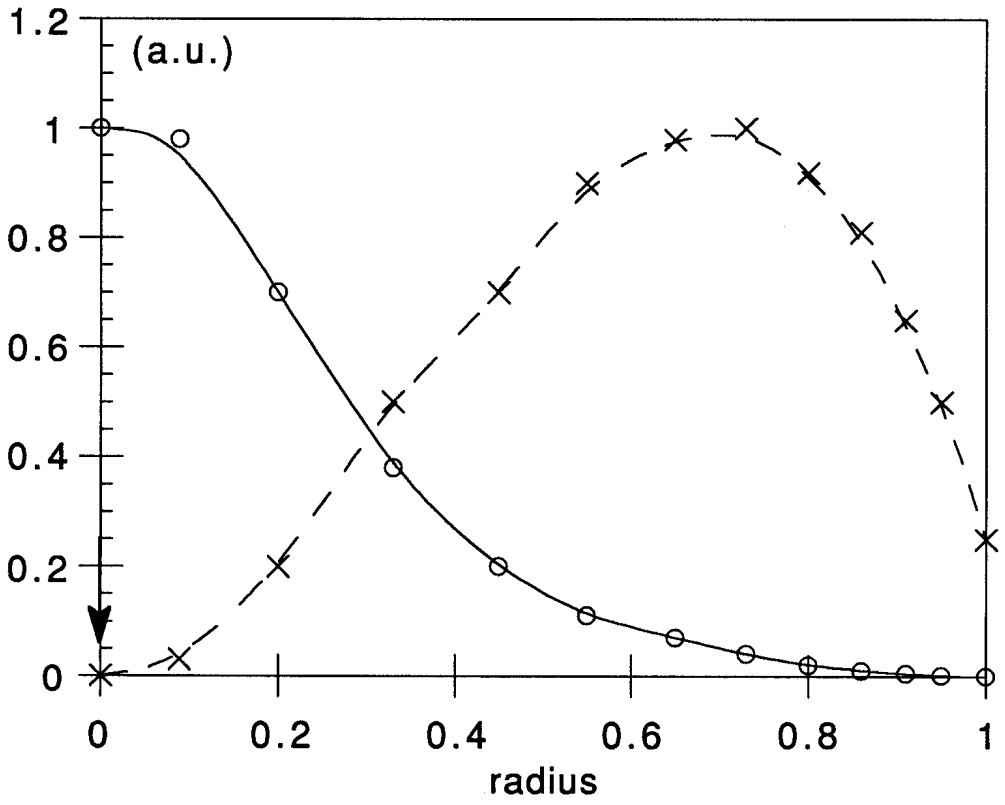

Fig.4

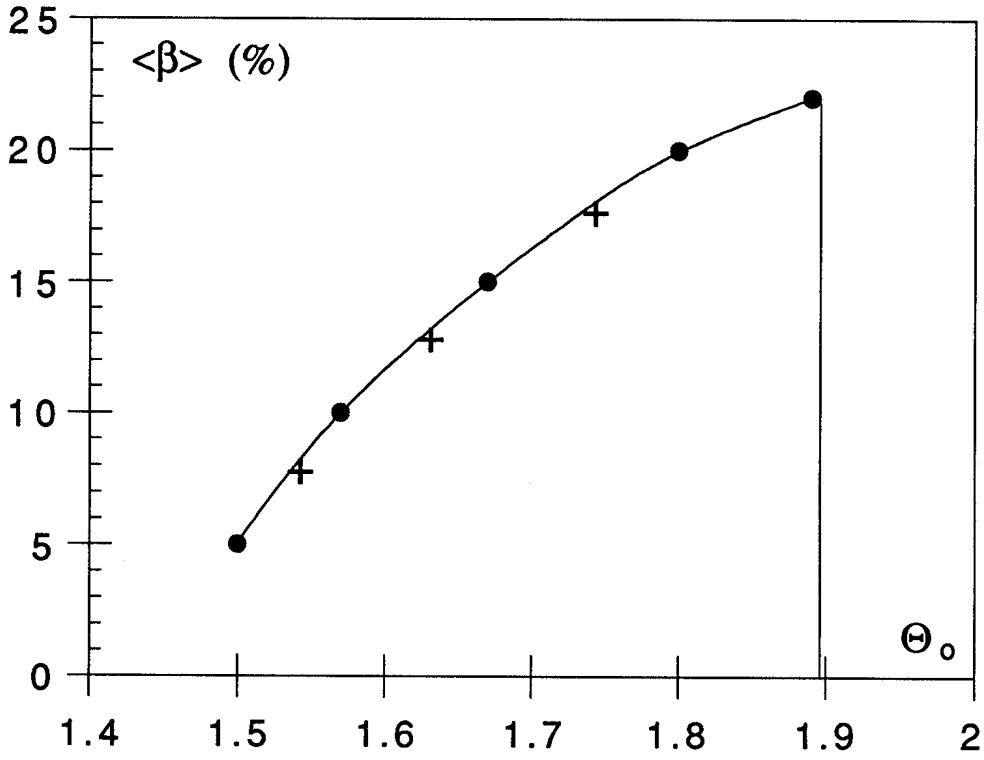

Fig.5

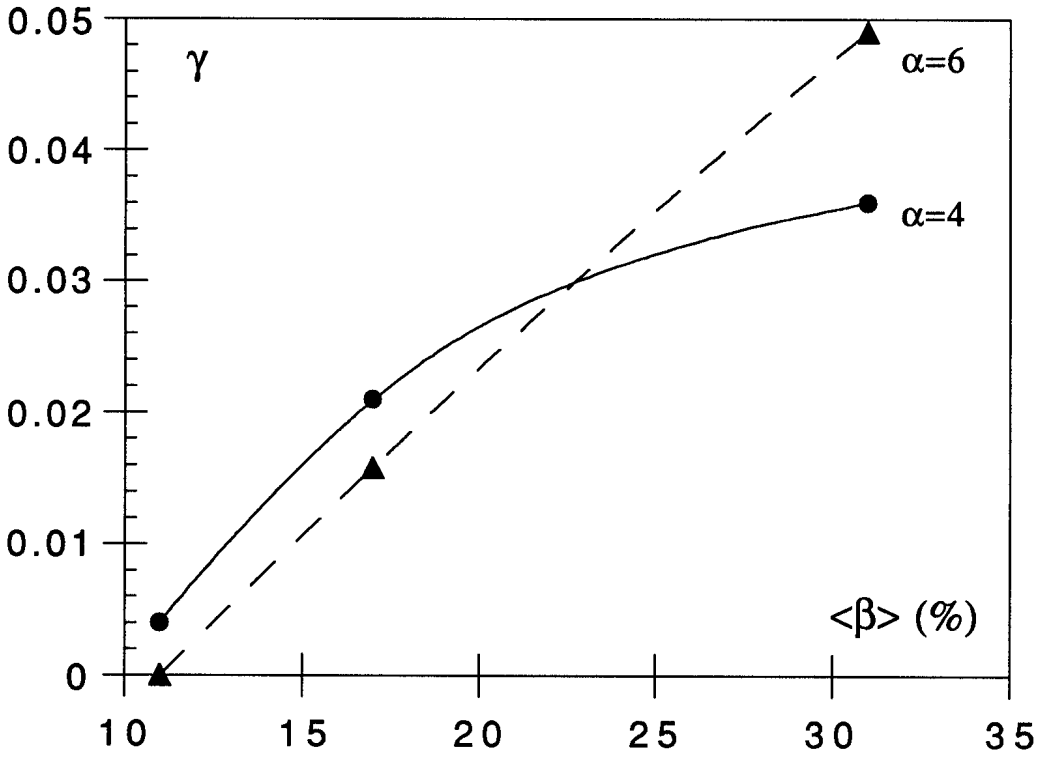

Fig.6

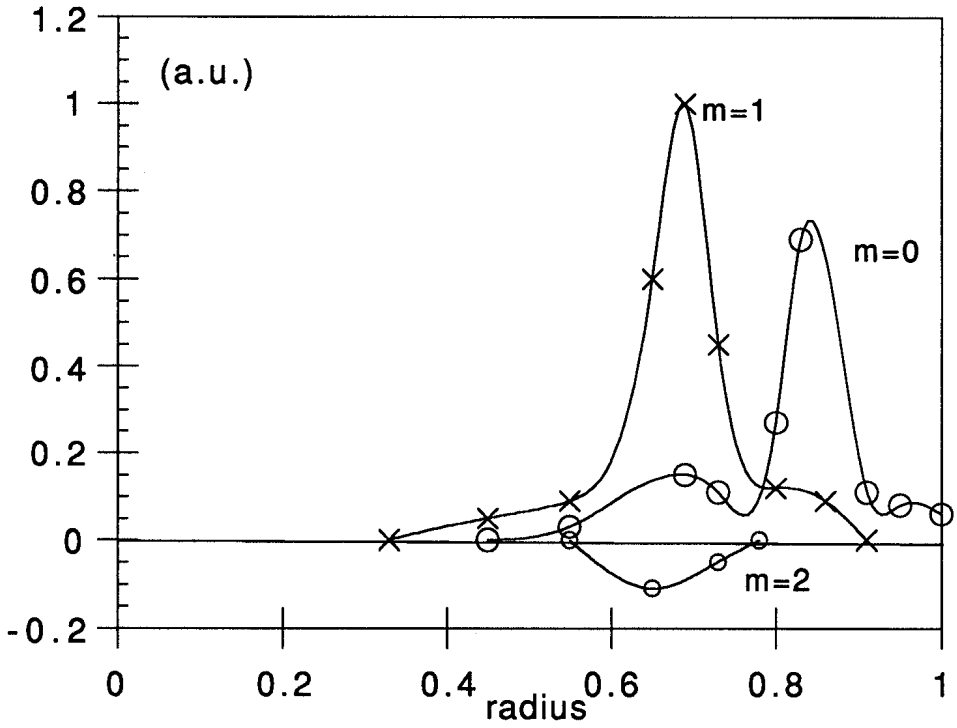
1.2
(a.u.)
1
0.8
0.6
0.4
0.2
0
-0.2
m=1
m=0
m=2
0
0.2
0.4
radius
0.6
0.8
1

Fig.7a

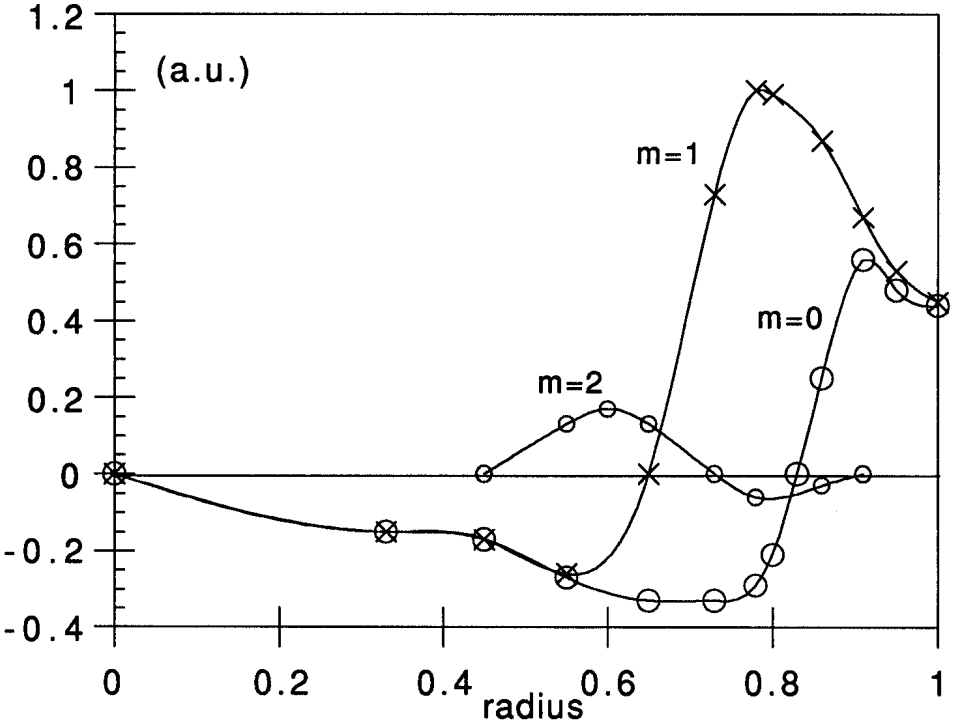
1.2
(a.u.)
1
0.8
0.6
0.4
0.2
0
-0.2
-0.4
m=1
m=0
m=2
0
0.2
0.4
radius
0.6
0.8
1

Fig.7b

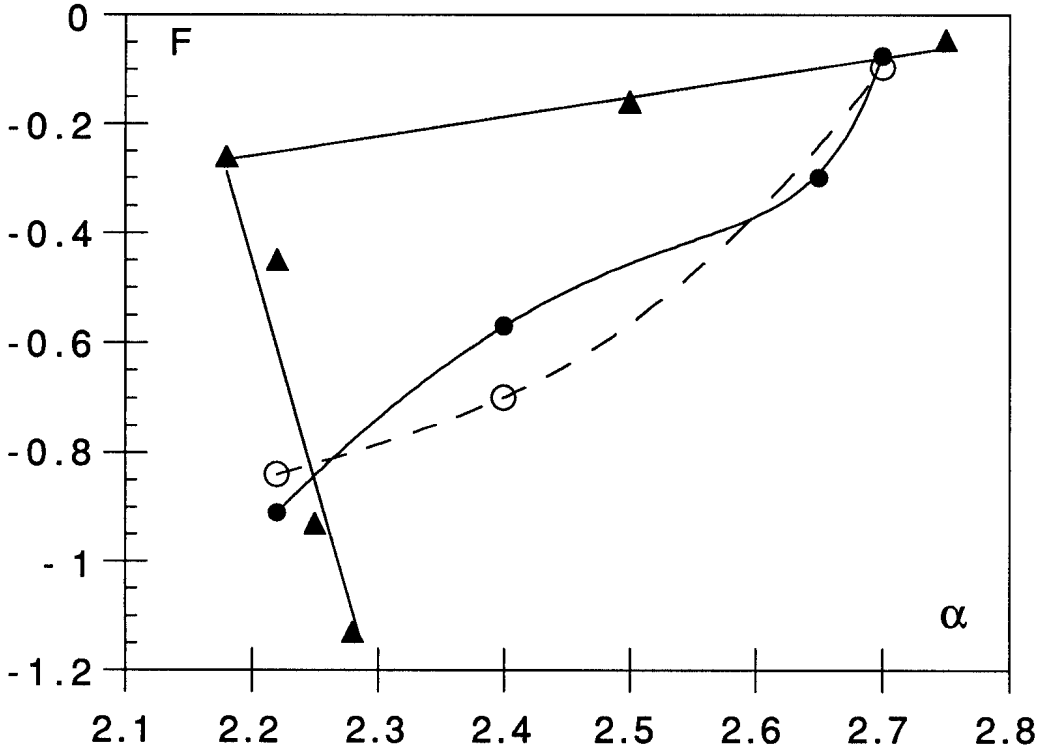

Fig.8

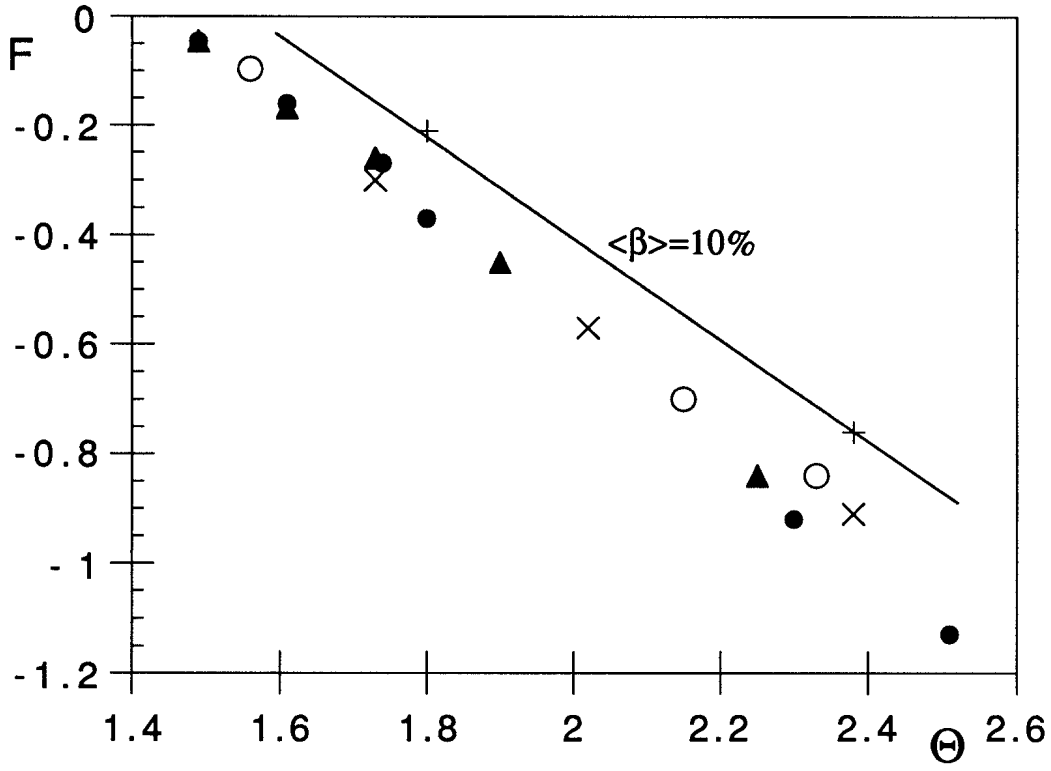

Fig.9

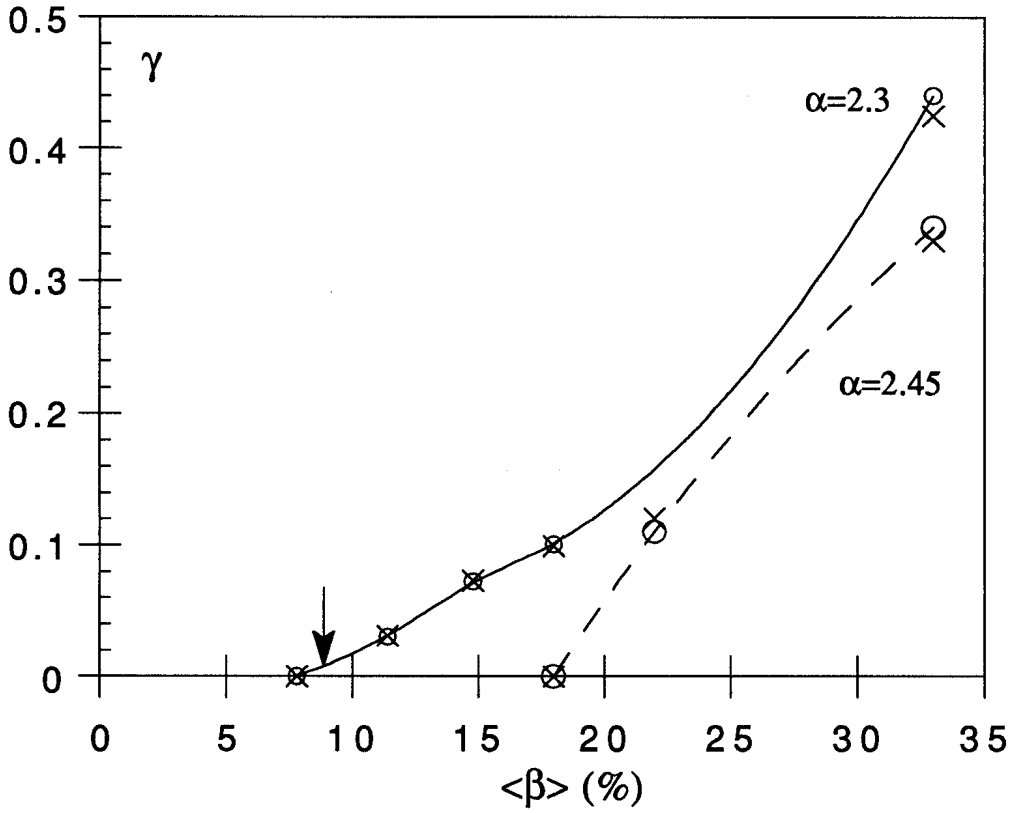

Fig.10

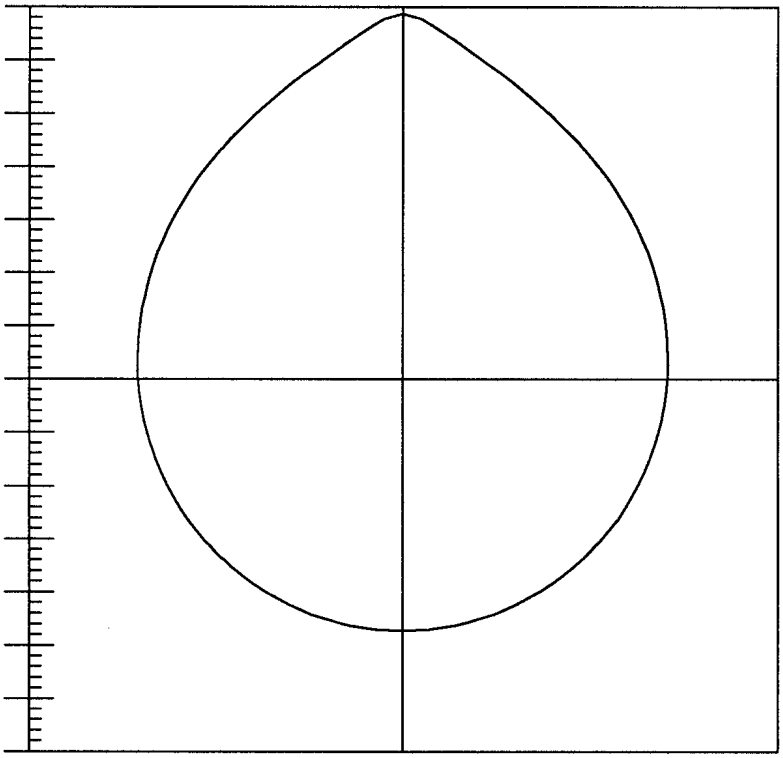

Fig.11

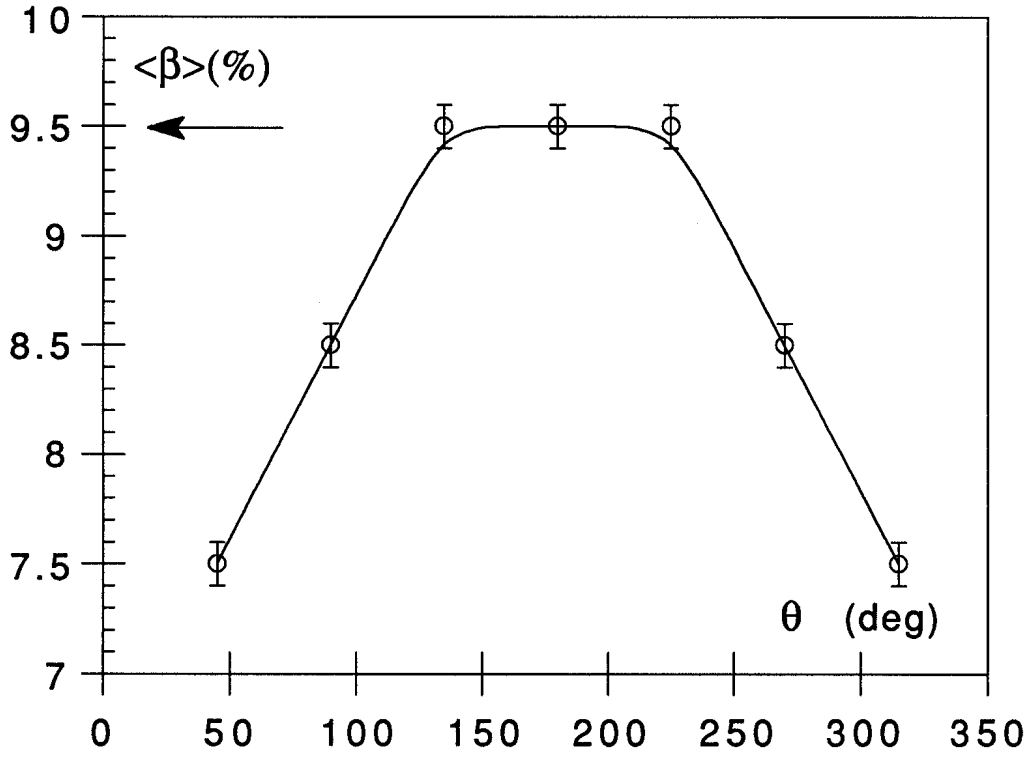

Fig.12